JOURNAL OF Materials CHEMISTRY

Water-dependent structural and chemical relaxation of bulk Co_3O_4 from cobalt nitrate decomposition

Mariangela Longhi and Leonardo Formaro*

Department of Physical Chemistry and Electrochemistry, University of Milan, Via Golgi 19, 20133 Milan, Italy. E-mail: formaro@icil64.cilea.it

Received 27th July 2000, Accepted 10th January 2001
First published as an Advance Article on the web 1st March 2001

The cell size of Co_3O_4 powders from exhaustively long cobalt nitrate decomposition (T=260–850 °C) is shown to depend on heating temperature and to expand upon prolonged room temperature ageing (1 year). By means of TGA and gas mass analyses, water from the starting salt is bound to the product oxide to various extents and is spontaneously released over time. Excess non-stoichiometric oxygen is left unaffected. A relation is observed between expanding cell size and decreasing bound water, suggesting that water is dissociatively accommodated in the lattice. The result is not within current defectivity models for Co_3O_4.

Introduction

Co_3O_4 is an effective catalyst in many gas–solid and liquid–solid reactions. Preparation is usually performed by thermal decomposition of cobalt salts, among which nitrate is often preferred due to decomposition temperatures as low as 200 °C. By changing the conditions, this feature allows highly dilute or thick and compact supported catalysts to be obtained, with little concern for substrate thermal stability. A literature survey showed that significant product features are seen to differ as if in response to uncontrolled or perhaps unexplored experimental factors, which is surprising given the widespread usage of this method. Unit cell sizes are the first area of concern. These reportedly vary with decomposition temperature and, remarkably, increase,[1,2] decrease[3] or remain constant[4] with heating temperature. This behaviour can be related to the acknowledged structural flexibility of spinels[5] and, in some cases,[1,2] is attributed to temperature-dependent variations in stoichiometry. This is a characteristic feature of Co_3O_4. The oxide can accept excess oxygen in the lattice[4,6–9] with respect to the nominal stoichiometry (O/Co = 1.33), thus originating a range of continuously varying compositions (Co_3O_{4+x}) relevant to catalytic applications. Moreover, the oxygen excess varies, decreasing with increasing temperature and eventually reaching nominal stoichiometry[4,6–9] at some limiting high temperature prior to thermal decomposition to CoO[10–12] ($T \approx 900$ °C). Thermal removal of excess oxygen is, however, reported to begin at around 350–450 °C,[13] or to be complete in a narrow temperature range around 800 °C,[1,4,14] which may be considered too widely divergent if the process is to represent a single, well-defined feature specific to oxide composition and structure. This viewpoint agrees with the literature. In a high-temperature XRD investigation[15] on structural Co^{2+}/Co^{3+} oxide disorder, available cell size results were preliminarily examined with respect to the preparative method used, with the result of highlighting extreme and likely abnormal values for Co_3O_4 specifically prepared by cobalt nitrate decomposition. As a result, the work was performed on Co_3O_4 from a different origin.

As a reaction involving phase transformation and matter exchange to and from adjoining phases, cobalt nitrate decomposition likely comprises several steps contributing to the features of the end-product. Reaction time and temperature have, as expected, obvious though unclear effects on reaction progress and product stoichiometry. Stoichiometric advancement is seldom considered, except by means of X-ray diffraction analysis of the product, so that no defined chemical criterion may be found on the behaviour (for different approaches, see: ref. 13, 16). This makes it doubtful whether the characteristic excess oxygen defectivity develops independently of cobalt nitrate conversion, or whether mixed interactions arise between the growing oxide and residual reactants from the starting salt. Nevertheless, it has been known for some time[17] that incomplete removal of nitrogen oxides (NO_x), and therefore reaction conversion, can affect catalytic oxide behaviour adversely. So far without proper consideration, it is also uncertain whether room temperature cell sizes represent equilibrium or slowly evolving states of the product oxide. Kinetic metastability is commonly encountered in thermal preparations, most often induced by end quenching procedures. In this case, some kind of relaxation may be expected to occur over time, which is perhaps a reason for the observed variability of Co_3O_4 from cobalt nitrate.

This paper deals with the behaviour of low surface area Co_3O_4 powders obtained at several temperatures while monitoring NO_x in carryover gases. Product characterisation was performed after *ca.* 15 days and then again 1 year after preparation.

Experimental

Low surface area Co_3O_4 powders (*ca.* 2–7 $m^2\,g^{-1}$) were obtained by a two-stage heating procedure. In the first stage, $Co(NO_3)_2{\cdot}6H_2O$ (Baker, reagent grade) was decomposed under O_2 flux (20 l h^{-1}, 5-nine O_2 from SIAD) for 18 h (T=190 °C). The product was made to react further at a higher temperature (T=260–850 °C) for 4+4 h with overnight intermediate cooling in flowing O_2. Glass or quartz vessels were used, depending on the temperature. Nitrogen oxides (NO_x) in carryover O_2 were accumulated for 2 h in 0.01 M KOH and then determined by acid titration. Experimental procedures are reported in detail elsewhere[18] and are outlined in the following section, as necessary, to describe some meaningful cobalt nitrate decomposition features. After final quenching to room temperature, samples were stored in dry, clean air. Results were obtained after *ca.* 15 days and then again after 1 year from preparation by means of XRD, TGA and mass analyses of thermally released gases.

X-Ray diffraction was performed by means of a Siemens D500 apparatus in a 2θ range from 10 to 70° (0.02° steps, 1 s

 DOI: 10.1039/b006095j

counting). Cell sizes were calculated by a standard least squares fit to the $\sin^2\theta$ values[19] of X-ray reflections.

Thermal gravimetry (TGA) was performed with a Perkin Elmer TGA7 instrument (O_2 flow, 5 °C min^{-1}). Mass analyses of thermally desorbed gases were obtained by means of a custom made instrument at 5 °C min^{-1} after degassing the sample for 1 h in flowing He at room temperature.

Results and discussion

Fig. 1 shows experimental diffractograms recorded shortly after preparation (*ca.* 15 days) on the first stage reaction intermediate ($T=190$ °C) and on a regular second stage product ($T=500$ °C). The angular peak positions of both samples are very close to one another and to the reference data.[20,21] No defined extra peak could be detected within the baseline noise, thus excluding foreign components. Moreover, similar and very narrow half-height peak widths were measured, and therefore large crystallite sizes were calculated (about 1500 Å), near the upper validity limit of the Scherrer equation. From these results, it would appear that highly crystalline and pure Co_3O_4 powders can be obtained under the conditions used, without readily detectable features related to differences in heating time and temperature. When compared with details in the NO_x release behaviour, this favourable picture becomes questionable and actually reveals a lack of sensitivity of X-ray diffraction with respect to impurity species. It is, at present, relevant that, at any constant temperature, NO_x release is not a smoothly decreasing function of time and varies with the heating regime adopted. For instance, after a sample is heated for some time at a constant temperature (*e.g.* 4 h, as in the second heating stage), the amount of NO_x accumulated in the alkali (during, for example, the last 2 h) is usually so small as to suggest that the reaction is complete within an arbitrarily fixed analytical sensitivity (2×10^{-4} M H^+ was used in ref. 18). However, NO_x can suddenly rise again to a high concentration if the sample is reheated under the same conditions after cooling to room temperature. Similar decreasing NO_x surges are most often observed through repeated heating–cooling steps on a particular sample. The samples in Fig. 1 therefore differ by (unknown) NO_x amounts released in the successive second stage heating steps.

For reasons which are, up to now, unexplained, cobalt nitrate decomposition can come to a standstill far from full stoichiometric conversion, with secondary species retained in large amounts in products from the starting salt, with these

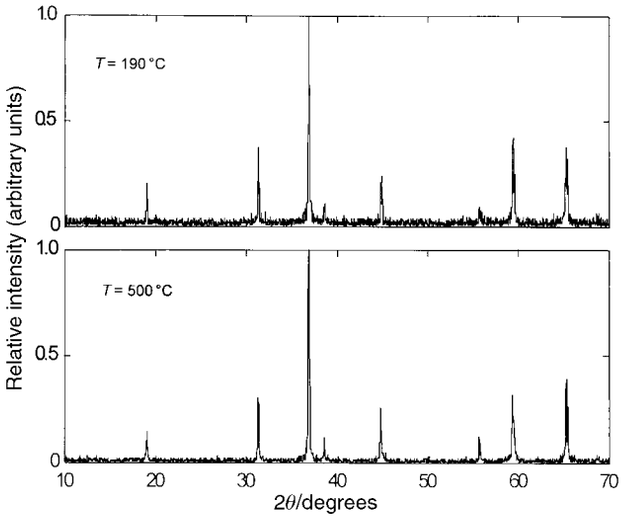

Fig. 1 X-Ray diffraction patterns for the first stage reaction intermediate ($T=190$ °C) and for a second stage end product ($T=500$ °C) after *ca.* 15 days ageing at room temperature.

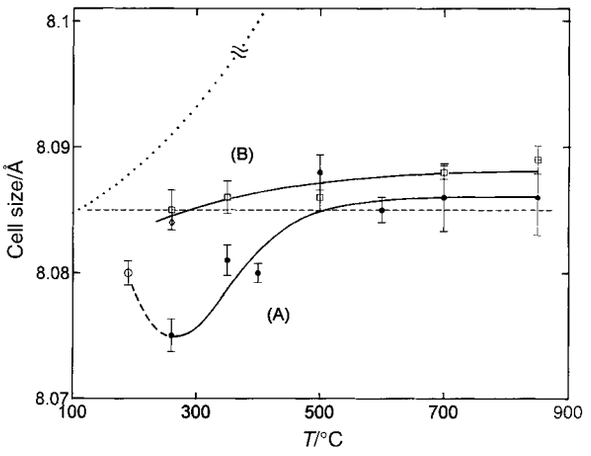

Fig. 2 Co_3O_4 average unit cell size and standard deviation as a function of reaction temperature. Lines (A) [filled circles (●)] and (B) [open squares (□)] are for second stage products at *ca.* 15 days and 1 year ageing, respectively. The first stage reaction intermediate ($T=190$ °C) is shown by the open circle (○). The horizontal line shows the adopted reference cell size from NBS data (see text). The dotted line shows *in situ* high-temperature diffraction results.[15,22] The lines are for visual guidance.

impurities remaining undetected by X-ray diffraction. This paper concerns Co_3O_4 from a preparation adjusted to obtain blank NO_x results in control heating of the second stage product from the lowest temperature used ($T=260$ °C).

Fig. 2 shows unit cell sizes as a function of reaction temperature and ageing time. Results are averaged over 8 meaningful peaks recorded for $10<2\theta<70°$; standard deviations are 0.003 Å at most (see error bars). For the sake of congruence, the adopted cell size reference, $a=8.085\pm0.002$ Å, is calculated averaging 8 values reported for the same 2θ range in the standard NBS diffraction data.[20] The value (see horizontal line in Fig. 2) is slightly higher than the overall average ($a=8.084$ Å), most often used for comparison in similar works. Control determinations were performed in an external laboratory.

After *ca.* 15 days from preparation (line A), regular second stage products show a trend of increasing unit cell sizes with increasing temperature, from sizes definitely more contracted ($T\approx260$–500 °C) to somewhat more expanded ones ($T\approx600$–850 °C), compared to the assumed reference. After 1 year of ageing (line B) the temperature-dependent trend shifts as a whole to more expanded values and becomes less steep, mainly due to stronger unit cell expansion of low temperature products compared to high temperature ones.

Ageing times and time effects have not been reported in previous papers. Any comparison must therefore concern unit cell sizes presumably determined shortly after preparation. A constant cell size ($a=8.095$ Å) is reported for $T=300$–450 °C on Ti-deposited Co_3O_4 coatings.[4] Conversely, the cell size of unsupported powders[3] is a fast decreasing function of temperature, from strongly expanded sizes ($a\approx8.097$ Å, $T=280$ °C) to more contracted ones ($a=8.077$ Å, $T=400$ °C) compared to the reference. Temperature-dependent, increasing patterns are reported for powders,[1,2] as in Fig. 2, starting from almost "normal" ($a\approx8.079_5$ Å, $T=240$ °C)[2] and extremely contracted ($a\approx8.038$ Å, $T=190$ °C)[1] low-temperature values, and reaching in both cases a high temperature quasi-plateau comparable with the present reference. Trends in variation are mostly uncommented upon. In ref. 1, cell size shrinkage with decreasing temperature was attributed to increasing excess oxygen defectivity. It is, however, apparent that, regardless of interpretation, specific structural features arise from the preparation, making any relation between cell size and heating temperature complex. This is in accordance with the above-

mentioned overview analysis,[15] which points to unresolved preparation effects. Complicating features are also observed in Fig. 2, where the first stage intermediate ($T=190\,^{\circ}C$) is clearly an outsider in the relevant short term pattern and features a unit cell much closer to the reference than other second stage products heated longer at higher temperatures.

Cell size expansion over time (Fig. 2) is considered straightforward evidence for product non-equilibrium, possibly imparted by previous heating or end quenching procedures. This topic is examined in further detail with reference to equilibrium (or near-equilibrium) Co_3O_4 cell sizes recorded *in situ* as a function of temperature (see dotted line in Fig. 2). This line shows a low-temperature section of almost coinciding cell size–temperature relations, independently recorded on Co_3O_4 powders of undisclosed origin equilibrated in air at both increasing and decreasing,[15] and just increasing[22] temperatures. A similar plot has been reported for Co_3O_4 films on Ti or quartz prepared using the method described above.[6] The Co_3O_4 unit cell size is therefore, in general, a rising function of temperature. On quenching, shrinking has to occur from any expanded cell size related to the particular temperature used. Given the characteristic temperature-dependent oxide composition,[4,6–9] the process comprises any cell size variation which may separately arise from purely physical thermal expansion, as for solids with constant composition and structure, and from a changing O/Co ratio. When, for instance, the sample temperature is decreased, the cell shrinks physically, while at the same time, molecular oxygen is absorbed from the atmosphere, ionised and then redistributed to the bulk to increase the equilibrium O/Co ratio related to the initial temperature. Structural readjustments would then result, possibly causing the cell to shrink more than in their absence, as proposed previously[1,2] to explain the temperature dependence of unit cell sizes of samples prepared using the present method. This further shrinking has been attributed[1] to an increase in electrostatic interactions between O^{2-} and cobalt ions promoted to a higher valence for local charge compensation, and to a decrease in the relevant cobalt radii. However, if equilibrium were to apply, shortly after quenching down to room temperature, a single, constant cell size would be recorded independently of heating temperature, and would be near the relevant value on the dotted line. This is actually in accordance with experimental results.[4] On inspection, the cell size would, moreover, be close to a well-established external reference, such as that adopted at present, and would correspond to any single-value maximum O/Co value higher than 1.33 imposed by room temperature equilibrium of excess oxygen defectivity. This shows that, if it is in any way related to excess oxygen, the unit cell shrinkage and exceedingly contracted unit cell sizes[1] observed with decreasing temperature[1,2] cannot be reconciled with equilibrium Co_3O_4 features. An O/Co value higher than the maximum required by room temperature equilibrium would be necessary.

It should be noted that cell size dependence on excess oxygen defectivity is still open to question. On the one hand, almost indistinguishable cell sizes[22] were recorded on Co_3O_4 equilibrated in air and pure O_2 ($T\approx100$–$800\,^{\circ}C$), although sample origin and defectivity were not reported. Given the defectivity dependence on oxygen pressure,[8] if confirmed in a wider O_2 range, this result would exclude any similar dependence for such samples. On the other hand, the cell size of mixed (Mg, Mn) spinel ferrites shrinks with increasing oxygen defectivity.[23]

Metastable states are commonly encountered in thermal preparations, mainly imparted by end quenching procedures. For fast quenching rates (in the work being uncontrolled), the sample temperature varies locally from place to place, causing expanded and contracted unit cells to coexist in nearby lattice domains. Structural mismatch, defects, strains, *etc.*, may develop, being eventually immobilised in room temperature products by at first decreasing and then completely ceasing lattice mobility. Shortly after cooling, more expanded cell sizes would, on average, result compared to what is required by room temperature equilibrium. Shrinking should spontaneously occur over time on recovery, and could be detected over a sufficiently extended experimental waiting time. This is contrary to the results given in Fig. 2 where, with the single exception at $T=500\,^{\circ}C$, after 1 year ageing, all cell sizes expanded to various extents, becoming greater with decreasing cobalt nitrate decomposition temperature. Equilibrium and non-equilibrium features related to thermal expansion and excess oxygen defectivity do not, therefore, influence the results shown in Fig. 2; presumably other processes, and species, are involved. Results are presented in Fig. 3 and 4.

Before concluding this section, it should be pointed out that thermal oxide behaviour may provide insights into the anomalous "stop and go" reaction progress, which is, so far, unexplained and most disruptive to the overall cobalt nitrate decomposition. As mentioned above, after heating at a constant temperature for some time, NO_x usually becomes negligible in carryover gases, rising again, however, to suddenly high concentration if an incompletely reacted yet crystalline sample, such as the first stage intermediate in Fig. 1, is reheated after cooling. Cracks or pores apparently open up by fast thermal expansion connecting bulk oxide regions with contacting gases and allowing entrapped species to be released faster than during the previous near to steady-state heating. This behaviour suggests that secondary product release is controlled by bulk diffusion within the solid and is further evidence for the variety of interactions taking place in cobalt nitrate decomposition.

Fig. 3 shows total weight losses $[(w_i-w_f)\times100/w_f]$ recorded by analytical TGA heating from room temperature (w_i) up to $T=850\,^{\circ}C$ (w_f). Starting from widely diverging values, higher for the less aged samples (line A) compared to those aged for the longer time (B), the weight loss values at first decrease with increasing temperature (to $T\approx500$–$600\,^{\circ}C$) and then reach a region of low, comparable values which, though scattered, outline a temperature-independent plateau. For reasons unknown, exceedingly large and scattered weight losses (*ca.* 8–12%) were recorded on the first stage intermediate after the shorter period of ageing and, therefore, the relevant point is omitted. No special feature was observed for the sample aged for 1 year, with weight losses averaging *ca.* 2% (see figure), in reasonable agreement with the temperature-dependent trend of other second stage products aged over extended periods of time.

The figure also shows the only results found in the literature

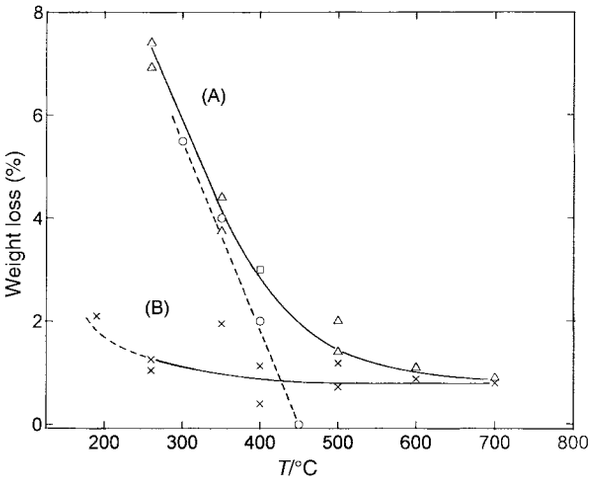

Fig. 3 Total Co_3O_4 weight losses as a function of reaction temperature. Lines (A) [crosses (×)] and (B) [open triangles (△)] are for *ca.* 15 days and 1 year ageing. Results from ref. 4 and ref. 11 are shown by the open circles (○) (see also the dashed line) and square (□), respectively.

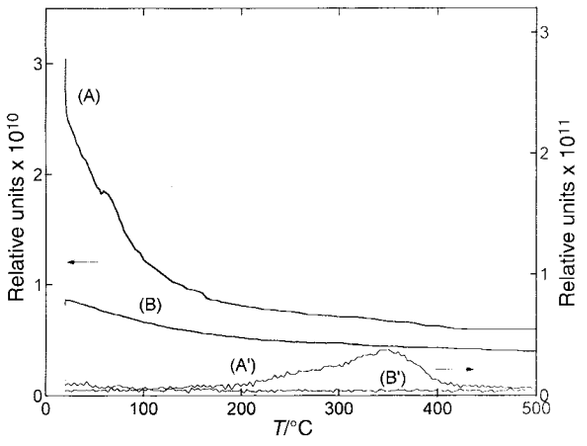

Fig. 4 Mass analysis of thermally desorbed gases from a second stage Co_3O_4 product ($T=260\,^{\circ}C$). Lines (A) and (B) are experimental water signals after *ca.* 15 days and 1 year ageing, respectively. Lines (A′) and (B′) are for similar NO results.

for Co_3O_4 powders[11] and layers on quartz[4] from similar preparations. A remarkable agreement is observed with the present short-term results, especially in the low temperature range (the $T=450\,^{\circ}C$ result is stated to be anomalous in the original paper).[4]

A relation is apparent between Fig. 2 and 3 in which cell sizes expand and matter is lost over time, by an extent which increases with decreasing cobalt nitrate decomposition temperature.

This relation cannot be identified further by TGA alone. In experimental traces, a sequence of ill-defined waves at variable peak positions is most often observed from room temperature to around 400–450 °C, and eventually overlaps with a better defined process extending from *ca.* 400 to 750 °C. This latter process is reproducibly observed in all cases, more clearly with increasing decomposition temperature and sample ageing. It is therefore intrinsic to the oxide behaviour and is consequently assigned to the transition from initially defective to near stoichiometric Co_3O_4 by excess oxygen thermal removal. This assignment is in accordance with the stability against weight losses observed at $T>750\,^{\circ}C$, where a flat, constant weight region occurs up to the maximum experimental temperature ($T=850\,^{\circ}C$) and before the thermodynamic decomposition limit of Co_3O_4 to CoO ($T\approx900\,^{\circ}C$, $p_{O_2}=1$ atm).[10] Thermal decomposition at 920 °C in air has been recently reported.[11,12]

Low-temperature weight loss processes were investigated by mass analyses of thermally desorbed gases. Water and NO were detected (Fig. 4). The sample is a second stage product from the lowest heating temperature used ($T=260\,^{\circ}C$). To the best of our knowledge, water interactions with the present "as prepared" oxide are only reported in ref. 11 (see the relevant point in Fig. 3).

After 15 days ageing (line A′), NO is desorbed by a well-defined maximum at 200–400 °C. One year later (B′), NO is absent or near analytical sensitivity. NO, or any related nitrogen species from the starting salt, is retained in the products in spite of the extended heating time. This result is in accordance with poisoning by "adsorbed NO_x"[17] reported for Co_3O_4 catalysts from a similar, though shorter preparation. NO spontaneously disappears upon room temperature ageing, showing that, though the details are unknown, Co_3O_4–NO interactions are reasonably weak, rather than strong as assumed previously[17] based on the finding that high temperature treatments in a vacuum ($T=450\,^{\circ}C$) were necessary to remove "adsorbed NO_x".

Greater amounts of matter (see change in the relative axis scale) are involved in thermal water desorption from both 15 day (line A) and 1 year (B) aged Co_3O_4. By comparison of the lines, Co_3O_4 undergoes a natural water loss which, for the conditions used, is likely released into the contacting atmosphere. Water and water loss may therefore be the basis of the temperature- and time-dependent cell size behaviour in Fig. 2. Water–oxide interactions become a concern with a few relevant features emerging from Fig. 4. For line A, thermal water desorption begins near room temperature and proceeds by a fast decreasing trend up to 150 °C, thus showing that weak species and almost continuously overlapping interaction energies are involved. Among these species, interstitial (capillary) and a few physical water forms are experimentally distinguished from the initial, almost vertical signal drop and the small separate maxima at higher temperatures. Thereafter, water desorption occurs at slowly decreasing, almost constant, rates up to, and beyond, the maximum available temperature ($T=500\,^{\circ}C$). From the line shape, there is in fact little doubt that water is still present and desorbing at $T>500\,^{\circ}C$. This is the characteristic temperature of incipient removal of non-stoichiometric excess oxygen revealed by TGA. Strong and very strong water–oxide interactions are therefore self-consistently established, approaching the binding energy of the anion lattice in the host compound. Excess oxygen can be accommodated into separate oxygen-rich Co–O surface phases.[24] However, from a crystallographic point of view, excess oxygen sites in the spinel lattice are indistinguishable from the normal ones in stoichiometric Co_3O_4.[25]

After extended ageing (line B), water desorption occurs all over the temperature range at slowly decreasing, much lower rates than prior to ageing. In comparison with line A, weakly and strongly bound forms of water are lost at room temperature. An almost continuous spectrum of overlapping energies is therefore indicated in the overall oxide–water interaction, with separation energies comparable to, or smaller than, the thermal energy relevant to room temperature. This aspect is independently evidenced by the featureless water desorption in line B. The spontaneous, room-temperature water release can be viewed as starting by initially depleting any weakly interacting and readily available water forms, which are then slowly replenished from the stronger ones by matter and place exchange processes, with low activation energies. In the absence of a similar interaction energy distribution, the initial fast signal decrease up to 150 °C (line A) would remain unexplained given the previous extensive sample heating at a higher temperature ($T=260\,^{\circ}C$). Moreover, room temperature water release would be restricted to weakly bound species, leaving the strongly bound species unaffected. In that case, very small or no cell size variation would be expected over time.

The widespread energy distribution of water–oxide interactions is likely the reason for the lack of TGA resolution. Unfortunately, this same feature prevents the identification of any relation between oxide–water and oxide–oxygen interactions. However, some insight can be obtained from the time dependence of the data. For limiting high temperatures ($T\approx500$–$700\,^{\circ}C$), the difference between short and long term results (Fig. 3) is nearly zero or barely positive. Therefore, a mass release process prevails in the matter exchange balance to and from the atmosphere, and is likely due to water loss, as in Fig. 4, contrasted with any opposite contribution from interacting atmospheric oxygen. Oxygen is adsorbed onto the oxide anyway, even at room temperature,[6] thus excluding time-dependent oxygen loss. On the other hand, room temperature oxygen adsorption, and absorption, are kinetically slow[6] and therefore presumably restricted to the build up of oxygen-rich layers at the outermost oxide surface.[6,13] Therefore, oxygen contributions to the matter exchange balance are likely small and negligible within the sensitivity of the present TGA results on low surface area samples. This outcome can be extended to all samples in Fig. 3, regardless of heating temperature. At the moment of quenching, the above high-temperature products are in fact expected to be near stoichiometry,[4,6–9] and should

therefore adsorb (absorb) atmospheric oxygen more effectively and extensively than other initially more defective samples from lower heating temperatures. This shows that bulk excess oxygen can be assumed to be constant over time, and that, therefore, although still likely affected by unresolved residual water, the long term results in Fig. 3 represent excess oxygen bound to the bulk oxide by preparation at each given temperature. The pattern in Fig. 3 agrees with widely accepted expectations from the solid state,[4,6–9] by which excess oxygen in Co_3O_{4+x} decreases with increasing temperature. As discussed above, this is a non-equilibrium state, frozen in from the previous heating by quenching procedures. Thus, bound water amounts correspond to the difference between short and long term weight losses. Though to a first approximation and with no separation possible between strongly and weakly interacting species, total bound water decreases from a huge initial maximum of *ca.* 5–5.5%wt at 260 °C to negligible values at 500–600 °C.

Despite some indeterminate points arising from a comparison with "wet" surface features, a voltammetric investigation performed on the same electrode materials supports this picture.[18] The charge ratio between well-resolved, quasi-reversible Co^{2+}/Co^{3+} and Co^{3+}/Co^{4+} redox systems was found to increase with increasing preparation temperature and to remain constant within experimental reproducibility for more than 1 year ageing. Water is lost while leaving essentially unchanged the surface oxygen defectivity imparted by preparation, which is assessed in voltammetry by the ratio of complementary Co^{2+} and Co^{3+} surface sites necessary for local charge compensation.

The cell size behaviour in Fig. 2 represents non-steady-state conditions of the spinel lattice which can accommodate variable water amounts, contracting and expanding in response to increasing and decreasing water content. Though impossible to determine quantitatively, strongly bound water is only relevant to this behaviour, though any weakly bound form is most important to ensure continuing water release, and cell size expansion over time. Relations with external reference cell sizes from other preparations become uncertain or coincidental, as for the well-established NBS and JCPDS standard data adopted at present, both of them relying on Co_3O_4 from cobalt fluoride decomposition.

Mechanistic details on the various ways water may interact with the bulk oxide are beyond of the scope of this work. However, the relation between contracting cell size and increasing water content suggests that water is dissociatively accommodated in the lattice as H^+/OH^-. An opposite relation could be expected in the case where water was distributed as a neutral species over interstitial positions, diluting matter and therefore expanding the original lattice unit cell for steric reasons. A gain in lattice energy and more compact packing may be qualitatively expected from H^+/OH^- distributed over, as yet unknown, lattice positions; inducing better electrostatic screening, more effective delocalisation of charge and, perhaps, previously unavailable hydrogen bonding among nearest neighbours.

However, some constraints are present in the above picture. The first is imposed by the cubic spinel symmetry which is preserved for unknown, but likely increasing, amounts of structural water bound into the lattice with decreasing preparation temperature. This is perhaps best illustrated by comparing the results of Fig. 1 which, as stated above, concern reaction products with widely diverging total bound water contents. This shows that structural water (*i.e.* H^+/OH^-) is either accepted in the lattice in small, hardly detectable amounts, or is accommodated at quasi-reticular positions such as to leave the overall crystallographic structure essentially unchanged. A second, and more demanding, constraint regards readjustments in the valence of pristine Co^{2+}, Co^{3+} and O^{2-} sites in the presence of H^+/OH^-. This brings about the need for a restatement of Co_3O_4 defectivity with respect to current models, where tetrahedral[7] Co^{2+} or octahedral[4,6,26] Co^{3+} are assumed to be promoted to higher valencies for the purposes of the charge compensation required by excess oxygen.

It can be pointed out that the above experimental basis and proposed interpretation have, so far, no counterpart in the Co_3O_4 literature. The weight loss results reported in Fig. 3 from previous works were entirely attributed to only one of the present non-stoichiometric species, either to water[11] or to excess oxygen defectivity.[4] To the best of our knowledge, the only similar results[27] concern the spinel λ-MnO_2. Independent samples of this compound were characterised by different TGA water losses (8.8 and 7.5%) and cell sizes (8.03 and 8.08 Å), the greater water content corresponding to the more contracted cell size. This is in accordance with the present relation between contracting cell size and increasing amounts of bound water.

Acknowledgements

Financial support from the Ministry of University, Scientific and Technological Research (MURST) and from the National Council of Research (CNR) is gratefully acknowledged. The late Mr. Claudio Maran at SAES Getters, Milan, Italy, is also acknowledged for having performed part of long term XRD measurements.

References

1 R. Garavaglia, C. M. Mari, S. Trasatti and C. De Asmundis, *Surf. Technol.*, 1983, **19**, 197.
2 D. L. Caldwell and M. J. Hazelrigg, in *Modern Chlor-alkali Technology*, ed. M. O. Coulter, Ellis Horwood, Chichester, 1980, p. 121.
3 M. El Baydi, G. Poillerat, J.-L. Rehspringer, J. L. Gautier, J.-F. Koenig and P. Chartier, *J. Solid State Chem.*, 1994, **109**, 281.
4 V. V. Shalaginov, I. D. Belova, Yu. E. Roginskaya and D. M. Shub, *Elektrokhimiya*, 1978, **14**, 1708.
5 R. J. Hill, J. R. Craig and G. V. Gibbs, *Phys. Chem. Mineral.*, 1979, **4**, 317.
6 I. D. Belova, V. V. Shalaginov, B. Sh. Galyamov, Yu. E. Roginskaya and D. M. Shub, *Russ. J. Inorg. Chem.*, 1978, **23**, 161.
7 J. H. De Boer and E. J. W. Verwey, *Proc. Phys. Soc., Extra Part*, 1937, **274**, 59.
8 A. Stokłosa and J. Zajęcki, *Solid State Ionics*, 1996, **91**, 315.
9 G. Tyuliev and S. Angelov, *Appl. Surf. Sci.*, 1988, **32**, 381.
10 E. Aukrust and A. Muan, *Trans. AIME*, 1964, **230**, 379.
11 E. Rios, G. Zelada, J. F. Marco and J. L. Gautier, *Bol. Soc. Chil. Quim.*, 1998, **43**, 447.
12 O. Knop, K. I. G. Reid, Sutarno and Y. Nakagawa, *Can. J. Chem.*, 1968, **46**, 3463.
13 Y. Takita, T. Tashiro, Y. Saito and F. Hori, *J. Catal.*, 1986, **97**, 25.
14 S. Angelov, E. Zhecheva and D. Mehandjiev, *Bulg. Acad. Sci. Commun. Dept. Chem.*, 1980, **13**, 369.
15 X. Liu and C. T. Prewitt, *Phys. Chem. Mineral.*, 1990, **17**, 168.
16 I. Nikolov, R. Darkaui, E. Zhecheva, R. Stoyanova, N. Dimitrov and T. Vitanov, *J. Electroanal. Chem.*, 1997, **429**, 157.
17 D. Pope, D. S. Walker and R. L. Moss, *J. Catal.*, 1977, **47**, 33.
18 M. Longhi and L. Formaro, *J. Electroanal. Chem.*, 1999, **464**, 149.
19 T. Pilati, private communication.
20 *Standard X-Ray Diffraction Powder Patterns*, NBS Circular No. 539, National Bureau of Standards, 1960, vol. 9, p. 29.
21 *J.C.P.D.S. Powder Diffraction File* **9-418**, International Centre for Diffraction Data, Swarthmore, PA.
22 B. Touzelin, *Rev. Int. Hautes Temp. Refract.*, 1978, **15**, 33.
23 S.-H. Kang, H.-I. Yoo and H. M. Park, *J. Mater. Res.*, 1999, **14**, 4070.
24 B. Marcus-Saubat, J. P. Beaufils and Y. Barbaux, *J. Chim. Phys.*, 1986, **83**, 317.
25 A. F. Wells, *Structural Inorganic Chemistry*, Clarendon Press, Oxford, 1967.
26 I. D. Belova, Yu. E. Roginskaya, V. V. Shalaginov and D. M. Shub, *Russ. J. Phys. Chem.*, 1980, **54**, 1016.
27 B. Ammundsen, P. B. Aitchison, J. R. Burns, D. J. Jones and J. Rozière, *Solid State Ionics*, 1997, **97**, 269.